Theory of Nanometric Optical Tweezers

Lukas Novotny, Randy X. Bian, and X. Sunney Xie
Pacific Northwest National Laboratory, P.O. Box 999, Richland, Washington 99352
(Received 14 January 1997)

We propose a scheme for optical trapping and alignment of dielectric particles in aqueous environments at the nanometer scale. The scheme is based on the highly enhanced electric field close to a laser-illuminated metal tip and the strong mechanical forces and torque associated with these fields. We obtain a rigorous solution of Maxwell's equations for the electromagnetic fields near the tip and calculate the trapping potentials for a dielectric particle beyond the Rayleigh approximation. The results indicate the feasibility of the scheme. [S0031-9007(97)03687-9]

PACS numbers: 42.50.Vk, 33.80.Ps, 41.20.Bt, 78.70.–g

Optical trapping by highly focused laser beams has been extensively used for the manipulation of submicron-size particles and biological structures [1]. Conventional optical tweezers rely on the field gradients near the focus of a laser beam which give rise to a trapping force towards the focus. The trapping volume of these tweezers is diffraction limited. Near-field optical microscopy enables the optical measurements at dimensions beyond the diffraction limit and makes it possible to optically monitor dynamics of single biomolecules [2]. The potential application of optical near fields to manipulate atoms or nanoparticles has been discussed in Ref. [3]. In this Letter, we present a new methodology for calculating rigorously and self-consistently the trapping forces acting on a nanometric particle in the optical near field and propose a novel high-resolution trapping scheme.

The proposed nanometric optical tweezers rely on the strongly enhanced electric field at a sharply pointed metal tip under laser illumination. The near field close to the tip mainly consists of evanescent components which decay rapidly with distance from the tip. The utilization of the metal tip for optical trapping offers the following advantages: (1) The highly confined evanescent fields significantly reduce the trapping volume; (2) the large field gradients result in a larger trapping force; and (3) the field enhancement allows the reduction of illumination power and radiation damages to the sample.

High resolution surface modification based on the field enhancement at laser-illuminated metal tips has been recently demonstrated [4]. It is essential to perform a rigorous electromagnetic analysis to understand the underlying mechanism for the field enhancement. Our analysis is therefore relevant not only to optical tweezers, but also to other applications, such as surface modification, nonlinear spectroscopy and near-field optical imaging.

To solve Maxwell's equations in the specific geometry of the tip and its environment, we employ the multiple multipole method (MMP) which recently has been applied to various near-field optical problems [5]. In MMP, electromagnetic fields are represented by a series expansion of known analytical solutions of Maxwell's equations. To determine the unknown coefficients in the series expansion, boundary conditions are imposed at discrete points on the interfaces between adjacent homogeneous domains. Once the resulting system of equations is solved and the coefficients are determined, the solution is represented by a self-consistent analytical expression.

Figure 1 shows our three dimensional MMP simulation of the foremost part of a gold tip (5 nm tip radius) in water for two different monochromatic plane-wave excitations. The wavelength of the illuminating light is $\lambda = 810$ nm (Ti:sapphire laser), which does not match the surface plasmon resonance. The dielectric constants of tip and water were taken to be $\varepsilon = -24.9 + 1.57i$ and $\varepsilon = 1.77$, respectively [6]. In Fig. 1(a), a plane wave is incident from the bottom with the polarization perpendicular to the tip axis, whereas in Fig. 1(b) the tip is illuminated from the side with the polarization parallel to the tip axis. A striking difference is seen for the two different polarizations: in Fig. 1(b), the intensity

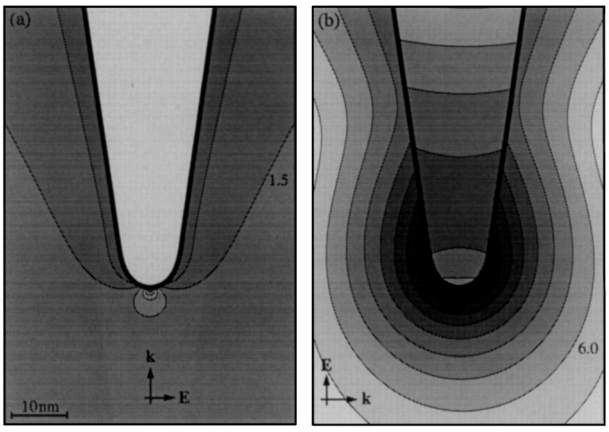

FIG. 1. Near field of a gold tip in water illuminated by two different monochromatic waves at $\lambda = 810$ nm. Direction and polarization of the incident wave are indicated by the **k** and **E** vectors. The figures show contours of E^2 (factor of 2 between successive lines). The scaling is given by the numbers in the figures (multiples of the exciting field). No enhancement at the tip in (a); enhancement of $\approx$3000 in (b). The field in (b) is almost rotationally symmetric in the vicinity of the tip.

enhancement at the foremost part of the tip is ≈3000 times stronger than the illuminating intensity, whereas no enhancement beneath the tip exists in Fig. 1(a) [7]. This result suggests that it is crucial to have a large component of the excitation field along the axial direction to obtain a high field enhancement. Calculations of platinum and tungsten tips show lower enhancements, whereas the field beneath a dielectric tip is reduced compared to the excitation field.

Figure 2 shows our calculation of the induced surface charge density for the two situations shown in Figs. 1(a) and 1(b). The incident light drives the free electrons in the metal along the direction of polarization. While the charge density is zero inside the metal at any instant of time ($\nabla \cdot \mathbf{E} = 0$), charges accumulate on the surface of the metal. When the incident polarization is perpendicular to the tip axis [Fig. 1(a)], diametrically opposed points on the tip surface have opposite charges. As a consequence, the foremost end of the tip remains uncharged. On the other hand, when the incident polarization is parallel to the tip axis [Fig. 1(b)], the induced surface charge density is almost rotationally symmetric and has the highest amplitude at the end of the tip. In both cases the surface charges form an oscillating standing wave (surface plasmons) with wavelengths shorter than the wavelength of the illuminating light. While the field enhancement has been calculated in the electrostatic limit [8], the presence of surface plasmons indicates that it is essential to include retardation in the analysis.

With the field distribution around the tip determined, the gradient force for a Rayleigh particle can be easily calculated as

$$\mathbf{F} = (\alpha/2)\nabla E^2, \tag{1}$$

where α is the polarizability of the particle [9]. The particle tends to move to the higher intensity region where its induced dipole has lower potential energy. The assumptions inherent in Eq. (1) are that the external field is homogeneous across the particle and that the particle does not alter the field $\mathbf{E}$ in Eq. (1). These assumptions, however, do not hold for a nanometric particle close to the tip as shown in our calculation (Fig. 3). The intensity contours are distorted around a dielectric sphere ($\varepsilon = 2.5$, 10 nm diameter) and the field inside the sphere is highly inhomogeneous.

To overcome the limitation of Rayleigh approximation, we performed a rigorous treatment of the trapping force by applying the conservation law for momentum [10],

$$\frac{d}{dt}\{\mathbf{G}_m + \mathbf{G}_{em}\} = \int_{\partial V} \mathsf{T} \cdot \mathbf{n}\, dS\,. \tag{2}$$

∂V denotes a surface enclosing the particle and $\mathbf{n}$ is the outwardly directed normal unit vector. The total mechanical and electromagnetic momenta inside ∂V are denoted by $\mathbf{G}_m$ and $\mathbf{G}_{em}$, respectively. T designates Maxwell's stress tensor given by

$$\mathsf{T} = \varepsilon_0\varepsilon\mathbf{E}\mathbf{E} + \mu_0\mu\mathbf{H}\mathbf{H} - \frac{1}{2}(\varepsilon_0\varepsilon E^2 + \mu_0\mu H^2)\,\mathsf{I}\,. \tag{3}$$

Here, I denotes the unit dyad and ε, μ are the dielectric constant and magnetic permeability of the surrounding medium, respectively. For time-harmonic excitation, the time average of $d\mathbf{G}_{em}/dt$ is zero and the net mechanical force can be expressed as [11]

$$\mathbf{F} = \left\langle \frac{d\mathbf{G}_m}{dt} \right\rangle = \int_{\partial V} \langle \mathsf{T} \cdot \mathbf{n} \rangle\, dS\,, \tag{4}$$

where $\langle \ldots \rangle$ denotes the time average. We find that for a particle in the vicinity of the tip, the magnetic contribution to the force is approximately 2 orders of magnitude lower than the electric one.

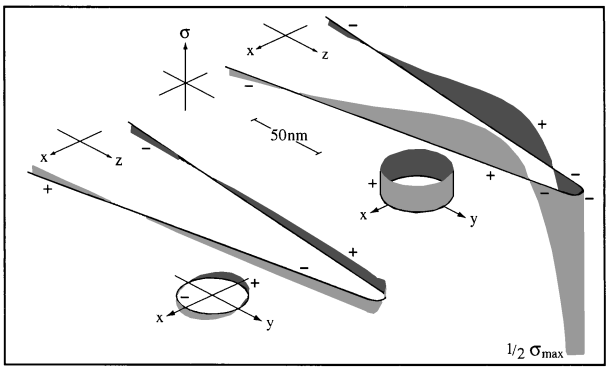

FIG. 2. Induced surface charge density corresponding to Fig. 1(a) (left) and Fig. 1(b) (right). The surface charges form a standing wave in each case. In Fig. 1(a), the surface charge wave has a node at the end of the tip, whereas in Fig. 1(b) there is a large surface charge accumulation at the foremost part, responsible for the field enhancement.

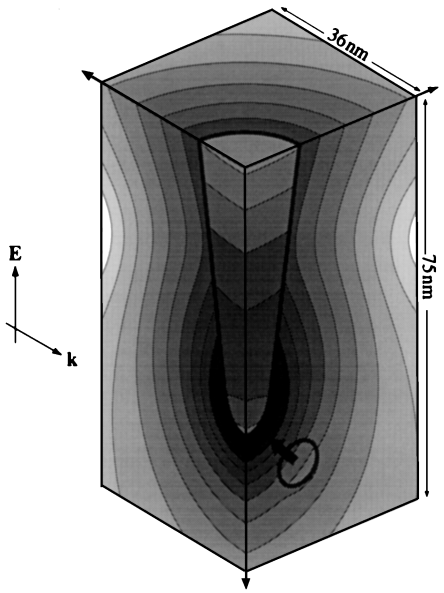

FIG. 3. Perturbation of the near field by a particle being trapped ($\varepsilon = 2.5$, 10 nm diameter). The field inside the particle is highly inhomogeneous, requiring rigorous calculation of the trapping force. The arrow indicates the direction of the trapping force. Same scaling as in Fig. 1(b).

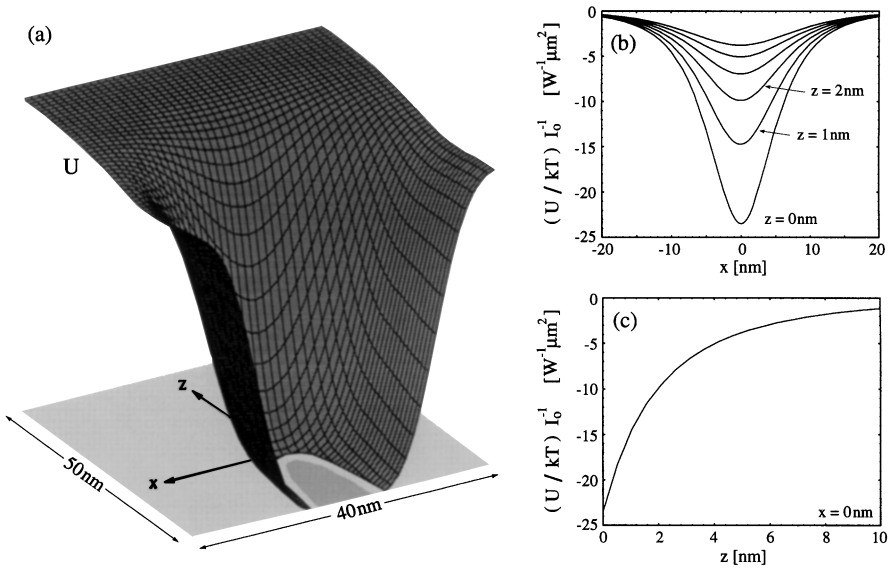

FIG. 4. Trapping potential of a particle ($d = 10$ nm, $\varepsilon = 2.5$) in the vicinity of the tip. (a) Potential energy surface in the (x, z) plane (the tip is indicated by the shadow on the bottom plane). (b),(c) Normalized potential energy evaluated along the x and z directions, respectively.

To obtain the force field, the calculation was repeated for different center positions of the particle. The trapping potential (U) of a particle located at $\mathbf{r}_o$ was then determined by

$$U(\mathbf{r}_0) = -\int_{\infty}^{\mathbf{r}_0} \mathbf{F}(\mathbf{r})\, d\mathbf{r}\,. \tag{5}$$

For a particle of diameter $d = 10$ nm, Fig. 4(a) shows the potential energy surface in the (x, z) plane determined from a grid of 40×50 positions. Figures 4(b) and 4(c) show cross sections of the trapping potential along the forward and transverse directions of the tip. Since the trapping potential is almost rotationally symmetric, we show only results for the (x, z) plane. The potential is normalized with the illuminating intensity I_0 and with kT (k = Boltzmann constant, $T = 300$ K).

The potential in the (x, y) plane is quasiharmonic near the potential minimum [Fig. 4(b)]. According to the theory of Brownian motion of a particle in a harmonically bound potential [12], the variance in the x direction near the potential minimum ($x = 0$) is given by

$$\langle x^2 \rangle = kT \left(\frac{\partial^2 U}{\partial x^2} \right)^{-1}. \tag{6}$$

A similar equation holds for the y direction. It follows that for a trapping accuracy of 5 nm ($\langle x^2 \rangle^{1/2}$ or $\langle y^2 \rangle^{1/2}$), Eq. (6) necessitates that $I_0 = 65\ \mathrm{mW}/\mu\mathrm{m}^2$. If the tip is placed in the focus of a diffraction limited beam of area $0.1\ \mu\mathrm{m}^2$, the required laser power is 6.5 mW, which is a nondestructive power level for nonresonant illumination.

The trapping potential is sensitively dependent on the curvature and material of the tip, as well as the size, shape, and dielectric constant of the particle being trapped. Smaller spheres require higher trapping power, because the polarizability of the particle scales with its volume. A sharper tip is preferred for trapping smaller particles. Although it is generally easier to trap larger particles, there is also an upper limit for the particle size. With a particle considerably larger than the tip radius, the rapidly decaying fields close to the tip affect only the nearest part of the particle's surface.

The highly inhomogeneous field near the tip also exerts a mechanical torque on the particle being trapped. This torque can be calculated from a conservation law for angular momentum, similar to Eq. (2). Our calculation showed that the resulting torque tends to align the long axis of an ellipsoidal particle towards the tip [Fig. 5(a)]. The final alignment of the particle, however, is dominated by the trapping potential (associated with the net trapping force). The alignment of the particle in Fig. 5(c) is shown to be more stable than that in Fig. 5(b). With its long axis perpendicular to the tip axis, a larger fraction of the particle's volume is immersed into the highly inhomogeneous field near the tip.

A practical concern for the proposed tweezers is laser heating of the tip. High temperatures could cause sample damage and induce convection at the surface of the tip. Accounting only for heat transport by conduction, the temperature distribution is determined by

$$\nabla \cdot (k_t \nabla T) - c_p \rho (dT/dt) = p_{\mathrm{abs}}\,, \tag{7}$$

where k_t, c_p, and ρ are the thermal conductivity, the heat capacity, and the specific density, respectively. For water we used the values $k_t = 0.61 \times 10^{-6}\ \mathrm{W}/(\mu\mathrm{m\,K})$, $c_p = 4.18\ \mathrm{J}/(\mathrm{gK})$, $\rho = 0.997 \times 10^{-12}\ \mathrm{g}/\mu\mathrm{m}^3$, and for gold we applied $k_t = 3.17 \times 10^{-4}\ \mathrm{W}/(\mu\mathrm{m\,K})$, $c_p = 0.129\ \mathrm{J}/(\mathrm{gK})$, $\rho = 19.3 \times 10^{-12}\ \mathrm{g}/\mu\mathrm{m}^3$. The source term, p_{abs}, denotes the absorbed power density given by the solution for the electromagnetic fields $p_{\mathrm{abs}} = (1/2)\ \mathrm{Re}\{\mathbf{j}^* \cdot \mathbf{E}\} = (E^2/2)\ \mathrm{Im}\{\varepsilon\}$, where $\mathbf{j}$ is the induced

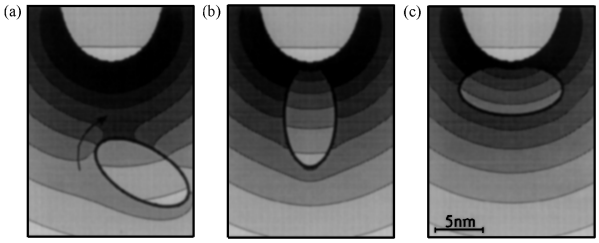

FIG. 5. Alignment of a prolate particle (long axis 10 nm, short axes 5 nm, $\varepsilon = 2.5$). (a) The field exerts a mechanical torque on the particle and tends to align its long axis towards the tip. Because the potential energy is lower for case (c) than for case (b), the particle is more stable when trapped with its axis transverse to the tip. Same scaling as in Fig. 1(b).

current density. We solved Eq. (7) numerically, using the finite difference time domain method [13]. Tip and environment were divided into $60 \times 60 \times 160$ cubic cells with a grid size of 4 nm. A time step of $\Delta t = 5 \times 10^{-17}$ s was used to ensure numerical stability.

Figure 6 shows the calculated steady-state temperature distribution for $I_0 = 65\ \mathrm{mW}/\mu\mathrm{m}^2$. ΔT is the temperature increase with respect to the original temperature (300 K, for example). A maximum of $\Delta T = 11.1$ K is reached inside the tip at the location of the maximum absorption [Fig. 1(b)]. The maximum value at the surface of the tip, however, is only $\Delta T = 6.5$ K. Note that ΔT scales to the illuminating intensity. Our result indicates that the temperature increase induced by laser heating is minimal for the intensity levels required for stable trapping.

In the proposed trapping scheme, a sharp metal tip is brought to the focus of an illuminating beam where a particle has been trapped by conventional means. A polarization component along the tip axis enables trapping of the particle to the near field of the tip. The trapped particle can be moved within the focal region of the illuminating light by translating the tip with a piezoceramic manipulator. The metal tip needs to be inert and nonreactive to the trapped particle. Then, the trapped particle can be released by turning off the laser illumination. The proposed scheme holds promise for nanometric manipulation of individual biomolecules in their aqueous environment.

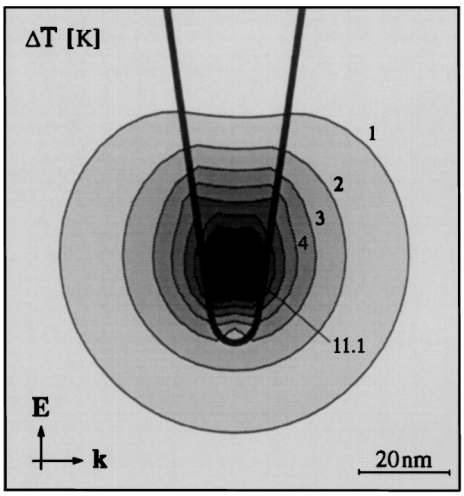

FIG. 6. Distribution of the temperature increase ΔT for an illuminating intensity of $I_0 = 65\ \mathrm{mW}/\mu\mathrm{m}^2$.

We thank Olivier Martin and Greg Schenter for helpful discussions. This research was supported by the U.S. Department of Energy (DOE). Pacific Northwest National Laboratory is operated for DOE by Battelle Memorial Institute under Contract No. DE-AC06-76RLO 1830.

Note added.—After submission of this Letter, an article by Martin and Girard on the field enhancement at pyramidal tungsten tips was published [14].

[1] A. Ashkin and J. M. Dziedzic, Science **235**, 1517 (1987), and references therein; S. Chu, Science **253**, 861 (1991).
[2] For reviews, see H. Heinzelmann and D. W. Pohl, Appl. Phys. A **59**, 89 (1994); E. Betzig and J. K. Trautman, Science **257**, 189 (1992); X. S. Xie, Acc. Chem. Res. **29**, 598 (1996).
[3] D. W. Pohl, in *Forces in Scanning Probe Methods*, edited by H.-J. Güntherodt, D. Anselmetti, and E. Meyer, NATO Advanced Study Institutes, Ser. E, Vol. 286 (Kluwer, Dordrecht, 1995), p. 235, and references therein.
[4] A. A. Gorbunov and W. Pompe, Phys. Status Solidi A **145**, 333 (1994); J. Jersch and K. Dickmann, Appl. Phys. Lett. **68**, 868 (1996).
[5] Ch. Hafner, *The Generalized Multiple Multipole Technique for Computational Electromagnetics* (Artech, Boston, 1990); L. Novotny, D. W. Pohl, and B. Hecht, Opt. Lett. **20**, 970 (1995).
[6] Since the tip size is still large compared to the mean-free path of the electrons in gold [see, C. F. Bohren and D. R. Huffmann, *Absorption and Scattering of Light by Small Particles* (Wiley, New York, 1983), p. 370], we believe that nonlocal effects are negligible.
[7] Different from a dielectric tip, we find that the intensity enhancement of a metal tip cannot be approximated by that of a single polarizable sphere, $4|(\varepsilon_2 - \varepsilon_1)/(\varepsilon_2 + 2\varepsilon_1)|^2$, ε_2 and ε_1 being the dielectric constants of tip and environment, respectively.
[8] W. Denk and D. W. Pohl, J. Vac. Sci. Technol. B **9**, 510 (1991).
[9] The scattering force can be neglected because of the small particle size and because there is no net radiation pressure associated with the evanescent fields close to the tip.
[10] J. A. Stratton, *Electromagnetic Theory* (McGraw-Hill, New York, 1941).
[11] J. P. Barton and D. R. Alexander, J. Appl. Phys. **66**, 2800 (1989).
[12] S. Chandrasekhar, Rev. Mod. Phys. **15**, 1 (1943).
[13] C. Temperton, J. Comput. Phys. **34**, 314 (1980).
[14] O. J. F. Martin and C. Girard, Appl. Phys. Lett. **70**, 705 (1997).